In Proceedings of the ISMA 2008 International Conference on Noise and Vibration Engineering, Leuven, Belgium, September 2008

Improved FRF estimators for MIMO Sine Sweep data

S. Orlando[1], B. Peeters[2], G. Coppotelli[1]
[1]Università di Roma "La Sapienza", Dipartimento di Ingegneria Aerospaziale e Astronautica
Via Eudossiana 18, 00184 Roma, Italy
e-mail: **giuliano.coppotelli@uniroma1.it**

[2]LMS International
Interleuvenlaan 68, B-3001 Leuven, Belgium
e-mail: **bart.peeters@lms.be**

Abstract
The dynamic identification of large aerospace structures like satellites, launcher components or aircraft prototypes, requires a great experimental effort in order to assure high quality test results. At the same time, because of the high development costs, a reduction of the test time is needed. In this paper, a test strategy capable to reduce the overall time required to perform dynamic tests aimed to the estimate of the Frequency Response Functions, FRFs, is introduced. A sine sweep excitation is the key point of the approach because of the good compromise between the excitation level and the testing time. Nevertheless, the accuracy of the dynamic identification strongly depends on the non-parametric estimation method used to compute the FRFs from the sine-sweep input-output data. In this paper, the accuracy of the estimates of both the frequency response functions and the modal parameters due to different sweep rates and different FRF estimation methods will be analyzed. These methods include: harmonic estimator, single-block Discrete Fourier Transform (DFT), frequency averaging technique, Welch's method and Reduced Discrete Fourier Transform (RDFT). The performance of the different estimators is critically assessed by a numerical analysis performed on a lumped parameter system and by experimental investigations carried out on both a GARTEUR aircraft scaled model and the Lambert aircraft M212.

1 Introduction

Ground Vibration Tests (GVTs) are modal tests conducted to investigate the dynamic behavior of the aircraft. They are necessary to make reliable flutter predictions, to validate and update the mathematical model of the aircraft, and for the certification process. These tests are usually scheduled before the maiden flight, during a period of extreme time pressure due to the testing of the fully assembled prototype. Because of the high development costs, the industry is calling for a significant reduction of the testing period. At the same time, it is indispensable to improve the existing test methods and to adapt new ones to the very specific needs of aerospace [1] in order to best fulfil the industrial requirements for each specific prototype undergoing a modal test. Likewise, the data analysis needs to be available as quickly as possible. Therefore, this trade off between extended measurement specifications required achieving better results on the one hand and the industrial call for a reduction in test duration on the other, reveals a great need for more powerful methods combined with an improved test strategy [2]. For more than 3 decades, the use of the phase resonance method or so called normal mode testing has been almost exclusively required for large aerospace structures [3][4]. It is known to be the most accurate method for a good identification on large structures, but the main drawback is that it is a very time consuming test procedure. Therefore, the phase resonance method has been complemented, and partially substituted, by the so called phase separation techniques that find the aircraft modes starting from the frequency response functions and by applying modal parameter estimation methods. The idea is that most modes are extracted from a phase separation technique, whereas the critical modes (i.e. modes that show nonlinear behaviour, critical

modes for flutter prediction or modes that differ from analytical predictions [4][5]) are identified on the base of the normal mode testing. Frequency response functions can be computed by using different excitation signals. In the last years sine sweep excitation gained considerable attention [1][6] for its intrinsic good compromise between magnitude of excitation (needed for large aerospace structure) and testing time. Furthermore, sine sweep has a good signal to noise ratio, peak to RMS ratio and since it is possible to control the frequency, the amplitude and the phase, it allows characterising non-linearities of the system under test [6]. From recent tests emerged that reliable FRFs and modal data from sine sweep test runs depend on the FRF estimation method used to estimate the frequency response functions [1]. In this article, different FRFs estimation method will be compared in order to obtain reliable functions and modal parameters with sine sweep excitation. The assessment is divided into three main phases. First a numerical simulation is carried out to study the effects of different parameters on the FRFs and to compare the estimated modal parameter to those obtained theoretically. Then a Ground Vibration Test (GVT) is carried out on a model of aircraft, the Garteur model, characterized, like the large aircrafts, by closed modes and a weak non-linear behaviour. Finally data from a GVT on a real aircraft, the Lambert M212, are analyzed and FRFs and modal parameters compared to those obtained with a burst random excitation.

2 Theoretical Background

The sine sweep excitation signal, $u(t)$, could be expressed as function of time by:

$$u(t) = A\sin\left[\varphi(t)\right] \tag{1}$$

where A is the amplitude and $\varphi(t)$ is the argument, phase, of the sine. The pulsation $\omega(t)$ of the sweep is calculated from the time derivative of $\varphi(t)$. Depending on the law with which the pulsation varies, it is possible to introduce different types of sine sweep. In the linear sine sweep, the pulsation is a linear function of the time:

$$\frac{\omega(t)}{2\pi} = f(t) = f_0 + \alpha t \tag{2}$$

where $f(t)$ is the instantaneous frequency, f_0 [Hz] the starting frequency and α [Hz/s] is the sweep rate, i.e. the "velocity" of the frequency. The duration, T, of the excitation (to which correspond the end frequency f_e) could be expressed as:

$$T = \frac{f_e - f_0}{\alpha} \tag{3}$$

The angular position $\varphi(t)$ could be achieved by time integrating (2), that is:

$$\varphi(t) = 2\pi\left(\frac{\alpha}{2}t^2 + f_0 t\right) + \varphi_0 \tag{4}$$

where φ_0 is the integration constant equal to the initial angle at $t = 0$. Another type of sine sweep excitation is the exponential sine sweep (sometimes the term "logarithmic sweep" is used instead) in which the frequency varies exponentially with time:

$$\frac{\omega(t)}{2\pi} = f(t) = f_0 2^{\beta t/60} \tag{5}$$

where β [oct/min] is the sweep rate. For this case, the duration of the excitation signal is given by:

$$T = \frac{60}{\beta\ln(2)}\ln\left(\frac{f_e}{f_0}\right) \tag{6}$$

The angular position is given by:

$$\varphi(t) = 2\pi\frac{60 f_0}{\beta\ln(2)}\left(2^{\beta t/60} - 1\right) + \varphi_0 \tag{7}$$

The first step to estimate the FRFs is the computation of the spectra of both the input and the output signals. This time-to-frequency transformation process could be performed using different methods. The single-block Discrete Fourier Transform (DFT), Frequency averaging technique, Harmonic estimator, Welch's method (also known as "Block Overlapping Technique"), and Reduced Discrete Fourier Transform will be briefly outlined in the following subsections. It is worthwhile to point out that these methods could be performed on data from sine sweep excitations regardless their type. Once the input and output data have been transformed into the frequency domain, the frequency response functions could be evaluated using the standard techniques, and the modal parameters could be gained by curve fitting the identified FRFs [6].

2.1 Single-block DFT

The input and the output spectra are obtained applying the DFT to one large, single block of time data that encompasses the entire sweep, resulting in a frequency resolution given by $\Delta f = 1/T$. The SISO FRF estimate is simply a division of the output by the input spectrum. In case of multiple inputs, multiple sweeps have to be used with different phase relations between the sweeps. The input power spectra $\hat{S}_{uu} \in C^{N_i \times N_i}$ and the cross spectra between the outputs and the inputs $\hat{S}_{yu} \in C^{N_o \times N_i}$ can be computed as:

$$\hat{S}_{uu}(\omega) = \frac{1}{N_s} \sum_{i=1}^{N_s} U_i(\omega)\, U_i^H(\omega), \quad \hat{S}_{yu}(\omega) = \frac{1}{N_s} \sum_{i=1}^{N_s} Y_i(\omega)\, U_i^H(\omega) \tag{8}$$

where $U_i(\omega) \in C^{N_i \times 1}$ are the input spectra (N_i is the number of inputs), $Y_i(\omega) \in C^{N_o \times 1}$ are the output spectra (N_o is the number of outputs), $\bullet^H$ denotes complex conjugate transpose and N_s is the number of sweeps with $N_s \geq N_i$. The MIMO FRF can be computed using the classical MIMO H1 estimator [6], in which the number of averages corresponds to the number of sweeps:

$$\hat{H} = \hat{S}_{yu} \left(\hat{S}_{uu} \right)^{-1} \tag{9}$$

2.2 Frequency averaging technique

The starting points are the power and cross spectra derived with the DFT method (8). The frequency averaging technique method basically consists of averaging these power and cross spectra over several spectral lines [7], in order to have a reduction of both the noise and the amount of data. The new frequency resolution, Δf_{red}, is related to the starting resolution Δf through the reduction factor R, defined by:

$$R = \frac{\Delta f_{red}}{\Delta f} \tag{10}$$

that indicates the ratio between the new and the old frequency resolution or in other words, the number of spectral lines that are averaged. The FRF calculation is then again performed according to (9).

2.3 Harmonic estimator

In this method, both the input and the output signals are divided into an integer number of periods, for example one, as reported in Figure 1 (Left), and the amplitude and the phase are estimated in a least square approach, step by step, for every period, under the assumption that the structure reaches the stationary conditions for each of the instantaneous frequency of excitation [8]. This complex envelope, with properties A, f_0, is then assigned to the middle instantaneous frequency of the considered time varying signal. Repeating this procedure for all the periods, an estimate of the actual amplitude and phase of the spectrum of the signal can be achieved. Note that this procedure identifies an approximated spectrum since the complex envelope is assigned to the instantaneous frequency. So the higher the sweep rate, the less valid this assumption will be. Once both the input and output spectra are estimated, it is possible to compute the auto-power and cross-power spectra and finally calculate the frequency response

function (9). Actually, in the LMS hardware [9] and software [10] implementation of the sine sweep method, the excitation frequency is actually stepwise varied [8], but without introducing a waiting time between the steps and by still satisfying the overall sweep time as specified in (3) or (6). Therefore, the differences with a true continuously varying frequency are very subtle.

2.4 Welch's method – Block overlapping technique

In this technique, the first step is to divide the time signals in N_b blocks, each formed by an equal number of sampling points $nfft$, Figure 1 (Right), in order to obtain a desired frequency resolution Δf_{red} [7][11] given by:

$$N_b = \frac{N}{nfft}, \quad nfft = \frac{1}{\Delta f_{red} . \Delta t} \tag{11}$$

Also in this case, the reduction factor R (10), could be used to reduce the amount of data. A Hanning window is applied to every block to reduce leakage. The application of the window causes to be weight down to zero the data at the beginning and end of the time records and, therefore, an attenuation of the spectral amplitude and an overestimation of the damping. The power and cross spectra are then computed according to (8), but with the number of averages being equal to N_b instead of N_s. The FRF calculations are performed in the classical way (9). A comprehensive study of optimal window selection and overlapping strategies for reducing the bias and variance of frequency-response function measurements can be found in [12].

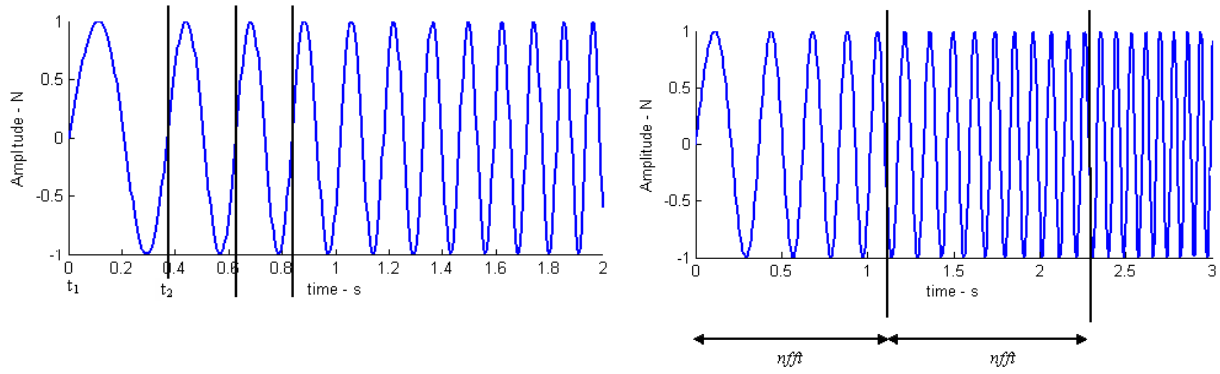

Figure 1: (Left) Input sine sweep and its division in an integer number of period. (Right) Division of blocks in order to have a desired frequency resolution.

2.5 Reduced Discrete Fourier Transform (RDFT)

Like in Welch's method, the first step is to divide the signals into N_b blocks, in order to obtain a desired frequency resolution [2]. At this stage, the reduction factor R is introduced. The time domain blocks are linearly averaged and the Discrete Fourier Transform is applied to the average of the blocks to obtain the spectra. The FRF calculation proceeds then as described in Section 2.1. It is interesting to observe that the RDFT method yields FRFs that are equivalent to selecting every R^{th} spectral line from the single-block DFT FRFs (Section 2.1).

2.6 Modal parameter estimation

Modal parameters are generally estimated from the minimization of an error function defined between the measured and the ones from the mathematical model. This minimization is carried out using a least-squares approach with respect to the unknown parameters. In this paper, the eigenfrequencies, damping

ratios and mode shapes are gained by using the PolyMAX frequency domain estimator [13][14] as implemented in Test.Lab [10].

3 Numerical analysis

In order to evaluate the behavior of the different estimators, a 6 degrees of freedom mechanical system is first introduced, Figure 2. Every mass m is equal to 10 kg except for node 3 which mass equals 30 kg, the spring stiffness k and the damper constant c are all equal to 150000 N/m and 60 N/(m/s) respectively.

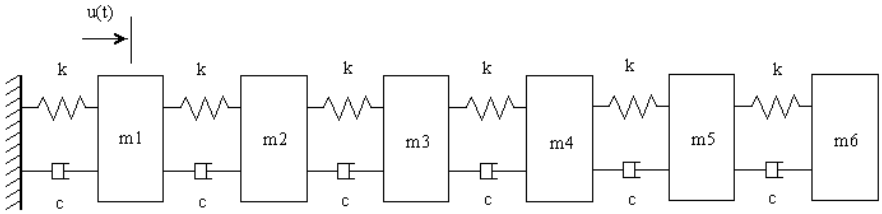

Figure 2: Lumped parameter mechanical system.

The reference modal parameters are calculated using a continuous-time state space model [15], and reported in Table 1. This model is then converted to a discrete-time state space model using the ZOH discretization method. From this last model the frequency response functions corresponding to the six outputs were evaluated. In Figure 3 the driving point FRF is depicted. These modal parameters and frequency response functions are considered as reference values/functions in the following numerical investigations, where the above mentioned estimators will be used to achieve the dynamic properties of the mechanical system when excited by a sine sweep loading.

Mode nr.	Frequency [Hz]	Damping [%]
1	3.9272	0.4935
2	13.5729	1.7056
3	18.0279	2.2654
4	28.1853	3.5419
5	32.2945	4.0582
6	36.2063	4.5498

Table 1: Modal parameters from model in Figure 2.

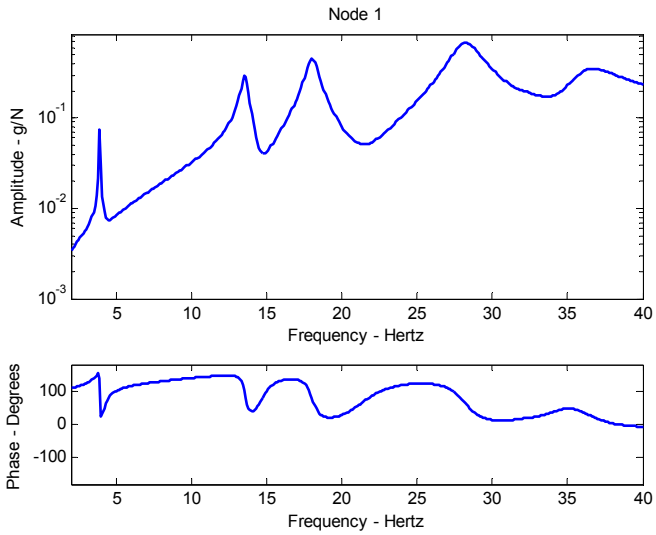

Figure 3: Driving point FRF from discrete-time state-space model.

3.1 Linear sine sweep and responses.

In order to analyze the influence of the sweep rate on the estimators, two linear sine sweeps with the same force amplitude but with two different rates, reported in Table 2, are considered. The driving point accelerations corresponding to the slow and the fast sweep rates are reported in Figure 4. When considering the slow sine sweep, it seems that the maxima of the responses are better identified with respect to the case of the faster sweep rate.

Moreover, such maxima occur with a time delay with respect to the time where the excitation frequency is equal to the resonant frequency of the system, as shown in Figure 5. It is worthwhile to remark that in this figure both the time domain response and the frequency response function are plotted in the frequency domain since the linear relation between the frequency of the excitation and the corresponding time (2). In the slow sweep case, the time delay for the maxima is higher in correspondence of the first modes which are the lower damped modes, see Table 1. When considering higher modes, this effect is less evident and the peaks of both the FRF and the response are coincident. Besides, the peaks are lower with respect to the previous case. So, the time delay is more accentuated for the lowly damped modes and increasing the sweep rate leads to accentuate this effect in the full covered range. The lower the damping ratio, the longer will be the transient and time to reach the steady state. If the velocity of sweep is high, the structure will not have time to reach the steady conditions because the transient is not died out yet when the frequency is varying.

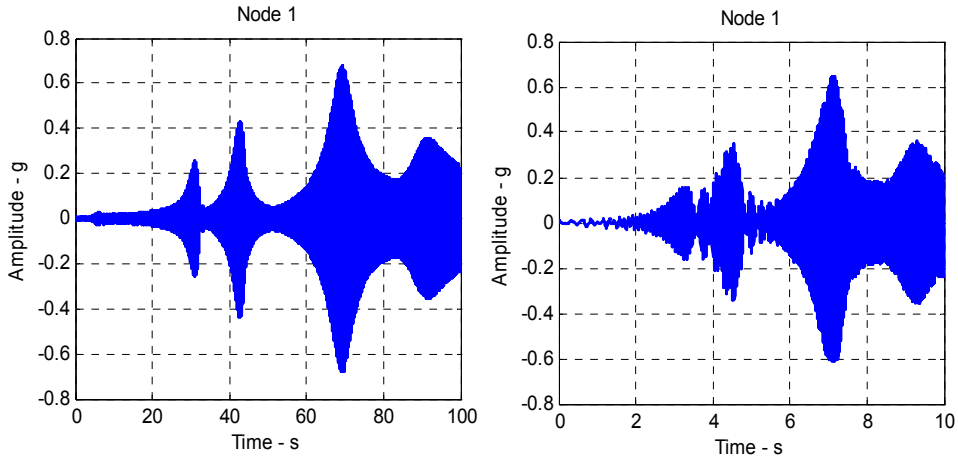

Figure 4: Response signals. Slow (left) and fast (right) sine sweep.

	Slow sine sweep	**Fast sine sweep**
Start freq. f_0	2 Hz	2 Hz
End freq. f_e	40 Hz	40 Hz
Sweep rate α	0.38 Hz/s	3.8 Hz/s
Sweep time T	100 s	10 s
Sampl. freq. f_s	200 Hz	200 Hz
Nbr. cycles N_c	2100	210
Nbr. of sampl. N_s	20000	2000

Table 2: Sine sweep characteristics.

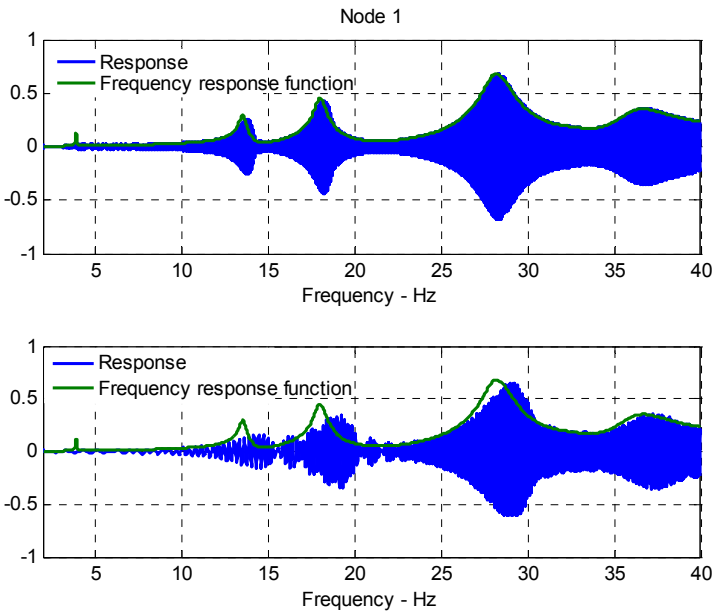

Figure 5: Effects of the sweep rate on the responses. Slow (top) or fast (bottom) sweep rate.

In order to make a realistic simulation, noise is added to the output signals. This is a zero mean random series with a 3% of standard deviation. Zeros are added on the input signals (zero padding) in order to avoid leakage in DFT, frequency averaging technique and RDFT methods. Since the slow sine sweep is characterized by a longer acquisition time, i.e., 20000 samples against 2000, more zeros are added on the

fast sine sweep in order to have the two simulations with the same frequency resolution. Figure 6 shows the amplitude of the FRFs achieved when exciting the structure with a slow sine sweep, $\alpha = 0.38$ Hz/s. Although the considered estimators are capable to give a good picture of the dynamic characteristics of the system, important differences have to be pointed out.

Regarding the harmonic estimator, it can be seen that the peaks of resonance are coarsely identified. The differences in the natural frequency estimates are remarkable for lower frequency modes, whereas it is acceptable for higher frequency. This is due to the fact that in correspondence of lower damping ratios the structure is not capable to reach the steady state conditions required by the methodology. Regarding the other methods, it can be seen that the RDFT leads to the more similar FRF to DFT method than Welch's and frequency averaging technique. This is caused by the different averaging mechanism of estimators that leads to different height of the peaks, especially at low frequency. The Welch's method yields the worst peaks: it suffers from biased estimation, due to the application of the windows that decreases when considering modes at higher frequencies. Instead, the frequency averaging technique leads to intermediate results between Welch's method and RDFT. The RDFT and specially the single-block DFT of the signals leads to noisier FRF than those computed with the other methods.

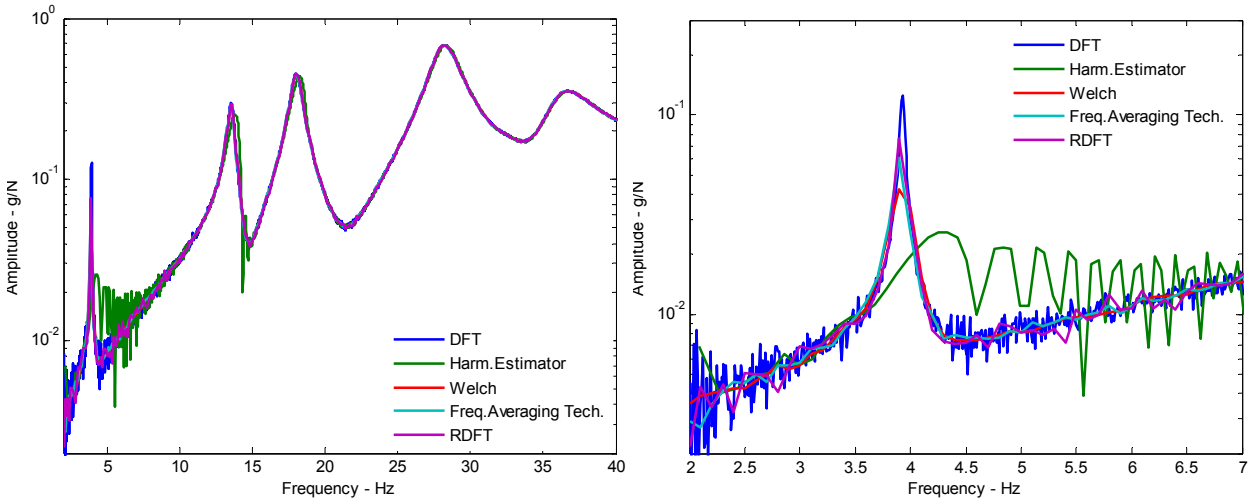

Figure 6: Comparison between the FRFs: Full range (left) and detail at low frequency (right). Slow sweep.

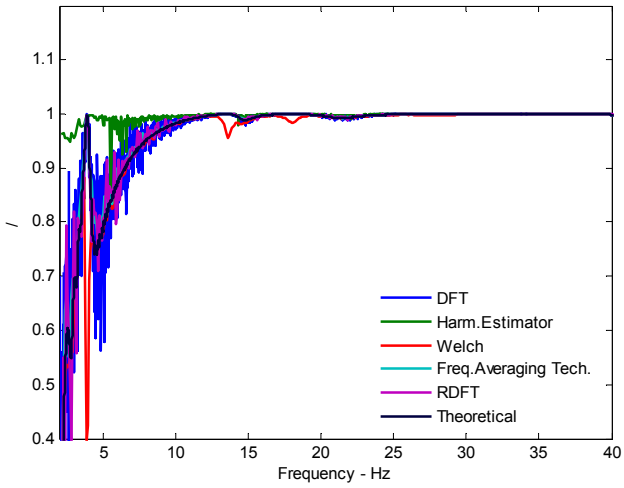

Figure 7: Coherence functions.

Also the coherence functions, reported in Figure 7, have a similar trend, except for the Welch's method and the harmonic estimator. The first one shows low values in correspondence of the resonances (maybe

due to leakage effects), whereas the harmonic estimator coherence presents oscillations at low frequency, without clean dip at the anti-resonance. Not all the coherences converge to the theoretical one that can be computed from the noise model used in the simulation, but only those computed with DFT, frequency averaging technique and RDFT.

Increasing the sweep rate (Figure 8) the harmonic estimator yields very distorted frequency response functions, specially at the lowly damped modes. The estimate of the first peak is completely wrong and also the high frequency peaks are wrongly estimated. The Welch's method yields a frequency response function that shows very high peaks, especially the first. This is caused by the fact that the block size is very large with respect to the total length of the signal, so the first window causes a big loss of information not recovered by overlapping. Increasing the frequency, this effect goes down. The other methods are not influenced by the sweep rate and the FRFs are equal to those obtained with the slow sweep. The coherence functions are not reported in this case, because they do not show relevant differences with those computed with the slow sine sweep. The modal parameters are then estimated from the frequency response functions computed using PolyMAX method (Section 2.6). The results for the 1st four modes are represented in Table 3 and Table 4.

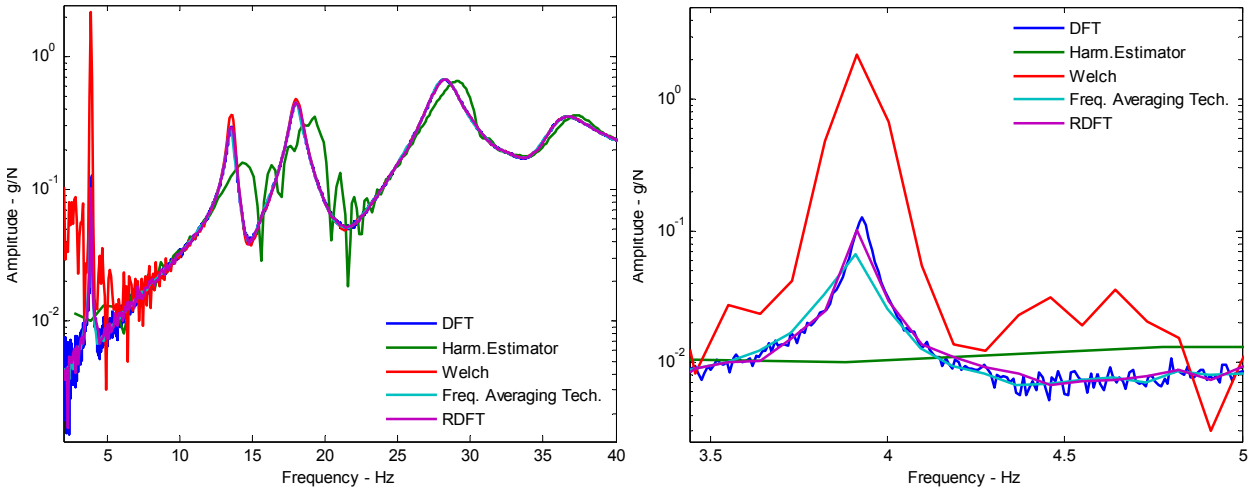

Figure 8: Comparison between the FRFs: Full range (left) and detail at low frequency (right). Fast sweep.

Mode	Harmonic Est.		DFT		Frequency av.		Welch's method		RDFT	
	Freq [Δ%]	Damp [Δ%]	Freq [Δ%]	Damp [Δ%]	Freq [Δ%]	Damp [Δ%]	Freq [Δ%]	Damp [Δ%]	Freq [Δ%]	Damp [Δ%]
1	**6.5**	**160.7**	0.0	0.0	0.0	**22**	0.1	**78.3**	0.0	**9.7**
2	1.2	**7.9**	0.7	0.0	0.0	1.4	0.0	**15.0**	0.2	-0.1
3	0.6	-3.7	0.0	0.0	0.0	-0.5	0.0	6.3	0.0	4.0
4	0.1	-0.5	0.3	0.0	0.0	0.0	0.0	1.9	-0.6	2.4

Table 3: Comparison of modal parameters with the theoretical ones. Slow sine sweep.

Mode	Harmonic Est.		DFT		Frequency av.		Welch's method		RDFT	
	Freq [Δ%]	Damp [Δ%]	Freq [Δ%]	Damp [Δ%]	Freq [Δ%]	Damp [Δ%]	Freq [Δ%]	Damp [Δ%]	Freq [Δ%]	Damp [Δ%]
1	**46.0**	**632.2**	0.0	-0.4	0.0	**23.6**	-2.8	**-29.1**	0.0	**9.3**
2	6.8	**129.2**	0.6	-0.1	0.0	2.2	-0.1	**22.3**	-0.1	0.4
3	4.7	**-33.8**	0.1	-2.3	0.0	-0.5	0.1	**10.4**	-0.2	1.9
4	1.6	**36.5**	0.4	-0.3	0.0	0.0	-0.1	**13.2**	0.0	0.4

Table 4: Comparison of modal parameters with the theoretical ones. Fast sine sweep.

The harmonic estimator yields great differences in the damping ratios estimates when considering the slow sweep, as reported in Table 3, specially at low frequency. Increasing the sweep rate, the estimation got worse wherever, although the DFT and RDFT method lead to the smallest differences with respect to the other methods, as reported in Table 4. The frequency averaging technique yields modal parameters that do not show relevant differences with respect to the theoretical ones, except for the first mode where the damping ratio is a higher than the theoretical one. Welch's method leads to an overestimation of the first mode damping caused by the application of the windows for the slow sweep rate case. An underestimation of the first damping ratio is reported with the fast sweep rate, due to, as already mentioned, the use of a larger data block size than the one required by the length of the signals.

4 GVT on Garteur airplane at SOPEMEA

A ground vibration test is carried out on the GARTEUR model, depicted in Figure 9, at the SOPEMEA laboratories, using exponential sine sweep. The free-free boundary conditions were simulated by hanging the test object with very soft springs. These suspensions are provided through a set of springs linked to a small plate between the fuselage and wing and to the concentrated mass on the fuselage. The response accelerations were measured at 21 nodes, evenly spread over the structure, for a total of 63 DOFs. The frequency range of the excitation loading was chosen equal to the one used in a previous test campaign [16], that is 5 – 65 Hz. Two electrodynamic shakers were used to excite the structure and two different shakers positions are analyzed: shakers located at intermediate wing points and shakers at the wing tips. In this work, just the analysis of the intermediate wing points measurements are reported. A slow, 1 oct/min, and a fast, 2 oct/min, sine sweep were used to excite the structure.

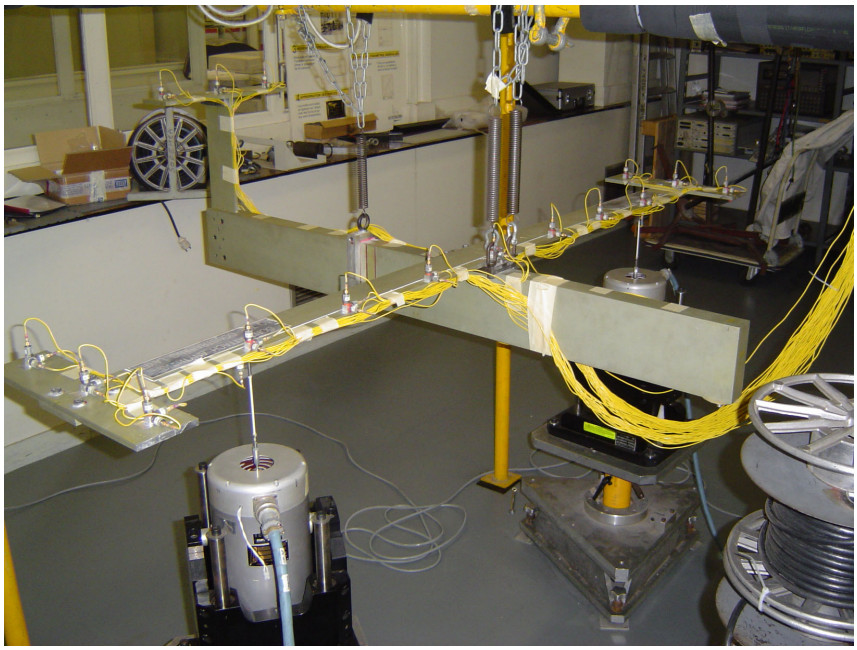

Figure 9: Measurement on GARTEUR model at SOPEMEA.

The resulting frequency response functions computed with the complete DFT of the signals, the online harmonic estimator (implemented on MIMO Swept Sine module of Test.Lab MIMO Sine), the offline harmonic estimator (implemented in the Matlab code to simulate the online harmonc estimator) are compared in Figure 10. Online and offline harmonic estimator show similar behavior and the resulting frequency response functions are practically the same. Relevant differences are found when considering the FRF computed with DFT. Looking at the low frequency range and specially at the first peak, it can be noted that the estimations are very different. The peak of the harmonic estimator is much lower and shifted

with respect to the one of DFT case. The former shows characteristic oscillations that have already been seen in the mechanical system analysis. Mismatches are visible at high frequency as well, but much smaller than those at low frequency. The frequency response functions computed with DFT, Welch's method, frequency averaging technique and Reduced Discrete Fourier Transform show a good correlation as depicted in Figure 11 (a reduction factor equal to 5 is chosen for the last three methods). Considering the first peak of resonance, a lower maximum corresponding to the Welch's method is reported. On the contrary, the DFT leads to the higher peak, whereas the frequency averaging technique is responsible of an intermediate peak level between the RDFT and Welch's approaches. At high frequency range, the curves coincide and no relevant differences were found. In Table 5, the modal parameters estimated using the sine sweep with 1 oct/min are shown. Modal parameters obtained from DFT method are considered as reference, since this method lead to the more reliable parameters, as reported in the numerical analysis section. The errors in the natural frequencies were practically immaterial for Welch's method, averaging technique and RDFT. Regarding the damping ratios, the biggest errors are in correspondence of the first mode. The Welch's method and the frequency averaging technique lead to a bigger error than the RDFT method. This difference is smaller for the higher frequencies modes. The harmonic estimator leads to the biggest errors, both on the frequency and on the damping ratios. From Table 6, where the modal parameters estimated using both the 2 oct/min and 1 oct/min sine sweep excitation rates are reported, it is confirmed that the harmonic estimator modes, are the most sensitive to the sweep rate.

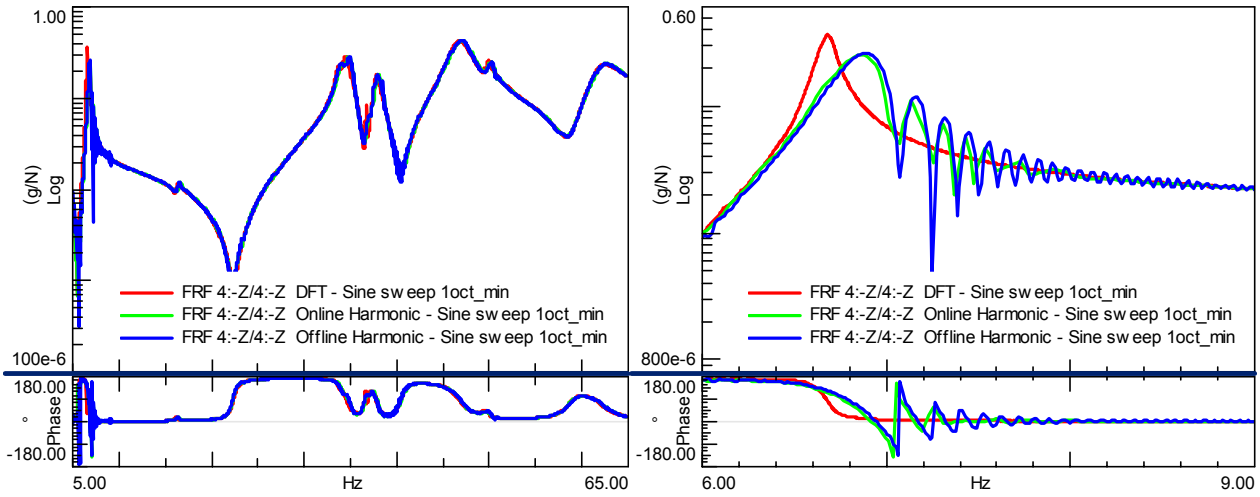

Figure 10: FRFs computed with DFT, online and offline harmonic. Full range (left). Zoom at low frequency (right). Sweep rate 1oct/min.

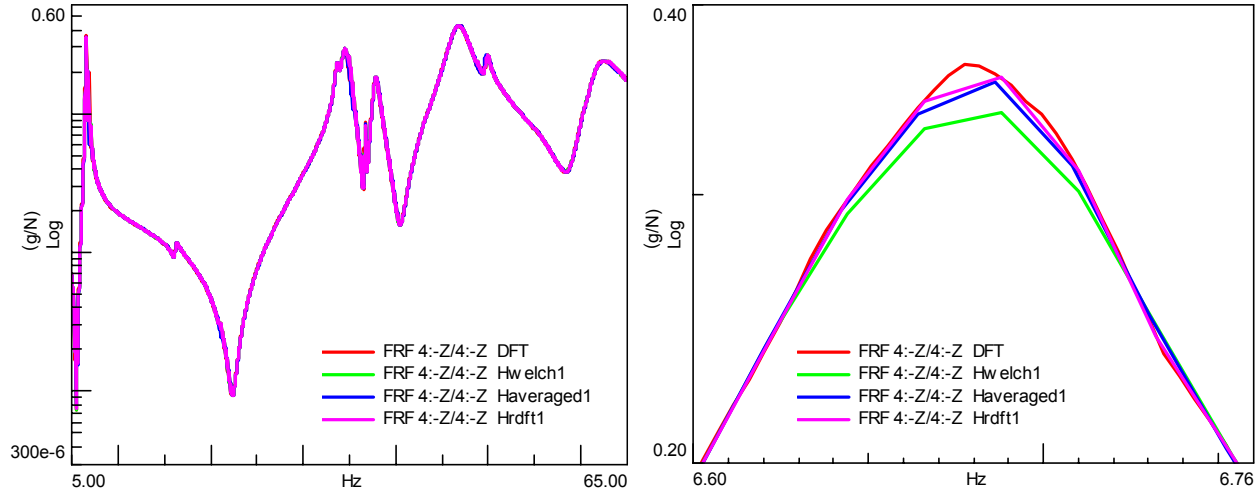

Figure 11: FRFs computed with DFT, Welch's method, frequency averaging technique, RDFT. R=5. Full range (Left). Zoom at low frequencies (Right). Sweep rate 1 oct/min.

Mode nr.	DFT		Welch		Aver.Tech.		RDFT		Harmonic	
	Freq [Hz]	Damp [%]	Freq [Δ%]	Damp [Δ%]	Freq [Δ%]	Damp [Δ%]	Freq [Δ%]	Damp [Δ%]	Freq [Δ%]	Damp [Δ%]
1	6.671	0.67	0.0	**22.4**	0.0	**16.4**	0.0	**9.0**	**8.1**	**70.1**
2	16.295	1.26	0.0	4.0	0.0	0.8	0.0	0.8	5.2	**36.5**
3	34.771	1.38	-0.1	1.4	-0.1	4.3	0.0	6.5	0.3	**28.3**
4	37.860	1.03	0.0	1.0	0.0	0.0	0.0	0.0	0.0	**19.4**

Table 5: Modal parameters. Comparison all methods with parameters obtained from DFT. Sine sweep 1 oct/min.

Mode nr.	DFT		Welch		Aver.Tech.		RDFT		Harmonic	
	Freq [Δ%]	Damp [Δ%]	Freq [Δ%]	Damp [Δ%]	Freq [Δ%]	Damp [Δ%]	Freq [Δ%]	Damp [Δ%]	Freq [Δ%]	Damp [Δ%]
1	0	-1.5	0.1	7.3	0.1	-4.3	0.1	-4.8	2.2	4.4
2	0	-0.8	0	4.6	0	1.6	0.1	-3.3	3.3	**44.8**
3	-0.1	6.7	-0.1	8.6	0	-6.9	-0.1	6.2	2	**29.3**
4	0	0	0	1	0	1	0	0	0.9	**11.4**

Table 6: Comparison modal parameter. Sine sweep 1oct/min vs sine sweep 2 oct/min.

5 GVT on Lambert aircraft M212

Finally, the sensitivity of the previously described estimators to the estimate of the modal parameters of the Lambert M212 aircraft (Figure 12) is investigated. The aircraft excitation was provided by both a burst random and linear sine sweep loading by two electrodynamic shakers placed one at the right wing and one near the tail in order to excite both the wing and the tail modes [17]. The excitation level of the burst random was equal to 3 RMS N, with a burst time equal to the 70% of the observation period, to allow the responses to decay to zero before the end of the observation time window, avoiding leakage. The sweep rate was set to 1 Hz/sec, for a duration of 85 sec. It is worth noting that the burst random excitation could be considered as a good reference input excitation because it is practically leakage-free, the noise could be easily removed by averaging the signals, and it is characterized by a fair signal-to-noise ratio. Therefore, useful information on the behaviour of the considered estimators could be gained by comparing the results achieved using both sine sweep and burst random. The test was performed on the aircraft in operational configuration with about 10 l fuel (only the hood was removed during the measurements). As for the GVT performed on the Garteur airplane, also in this case the free-free boundary conditions are adopted. For this case these conditions were obtained by removing the tires from the main landing gears and supporting the rims with flexible bungee. In addition, the aircraft was suspended at the engine mount instead of suspending it at the nose wheel. The number of the recorded experimental degrees of freedom were 110, but only data from 57 responses points, corresponding to the +Z local (vertical) direction were processed for the purpose of the paper. The frequency range was set so that the first fifty modes could be identified, that is 5 - 90 Hz, as described in [17], 1024 spectral lines, a sampling frequency of 200 Hz, and 40 averages were also considered.

A good correlation between the FRFs estimated by the complete DFT approach is reported in Figure 13, where the DFT approach is also compared with the online estimator actually available in LMS Test.Lab [10] (denoted as “online harmonic”). The harmonic estimator shows a good correlation with the DFT method at high frequency, whereas shifts in the peak of resonance and evident oscillations are reported for lower frequencies similarly to those previously identified when dealing with the GARTEUR model). The Welch’s method leads to a lower peak at low frequency with respect to the previous estimator, as depicted in Figure 14. Furthermore, the RDFT approach, with a reduction factor equal to 5, well approximates the FRFs achieved using the DFT and the burst random. At high frequencies there are no relevant differences.

Finally, the effects of the different frequency response function estimators on the estimate of the modal model are investigated. The estimate of the natural frequencies and the damping ratios is characterized by larger errors if identified with the harmonic estimator, as reported in Table 7. At low frequencies, the modal model identified from the frequency response function achieved using the harmonic estimator differs from the one estimated using the FRFs obtained by the other estimators, as depicted in the stabilization diagram and MvMIF of Figure 15 and Figure 16.

The identified modal model strongly depends on the excitation type and on the used estimator. The burst random excitation allowed the estimate of 46 modes, in the frequency range considered, regardless the estimation method. Nevertheless, using the sine sweep excitation, only 35 modes were identified by the harmonic estimators, whereas 43 modes could be identified by the other approaches.

Figure 12: GVT on the Lambert M212.

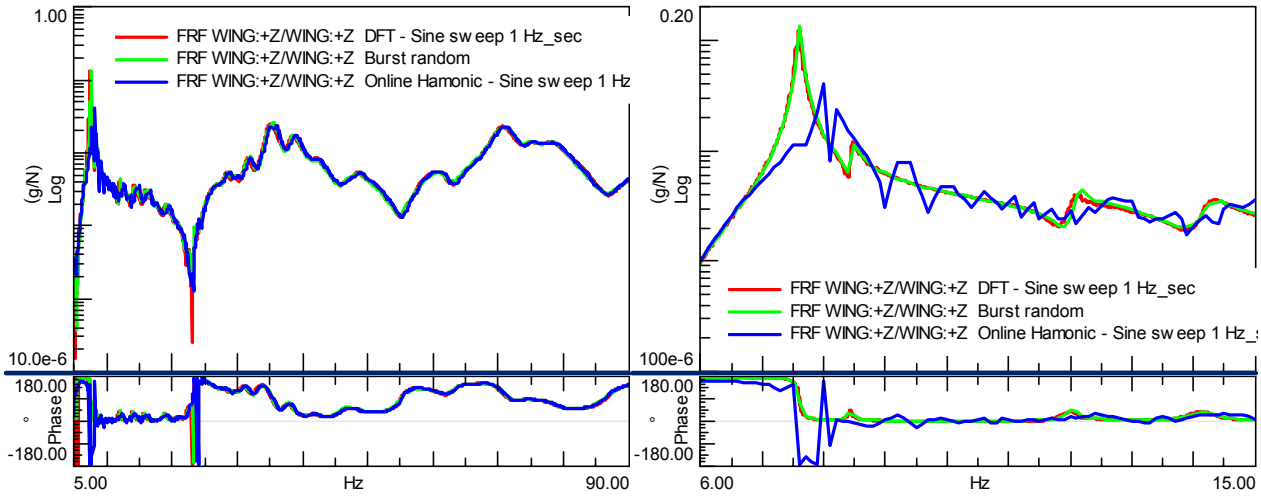

Figure 13: Comparison between the wing driving point FRFs: burst random and sine sweep processed with DFT and online harmonic (left). Zoom at lower frequency (right).

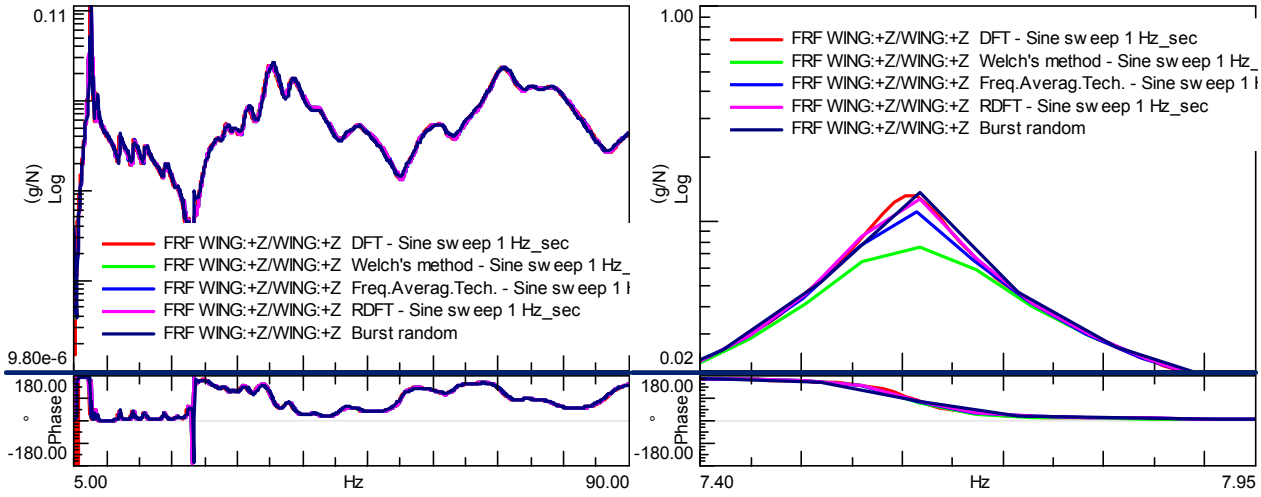

Figure 14: Comparison between the wing driving point FRFs: burst random and sine sweep processed with DFT, Welch's method, frequency averaging and RDFT, with R=5. Full range (left) and zoom at low frequency (right).

Mode nr.	Burst random		DFT		RDFT		Harmonic	
	Freq [Hz]	Damp [%]	Freq [Δ%]	Damp [Δ%]	Freq [Δ%]	Damp [Δ%]	Freq [Δ%]	Damp [Δ%]
1	7.608	0.478	0	0.023	0	0.03	0.556	0.329
2	8.459	0.604	0.003	0.045	0.004	0.034	0.67	1.674
3	10.238	0.236	-	-	-	-	-	
4	12.103	0.88	0.033	0.161	0.002	0.169	-	-
5	12.386	1.598	0.059	0.788	0.077	0.781	0.152	1.788
6	12.830	1.511	0.002	0.102	0.015	0.147	-	-

Table 7: Mode identified from burst random signal (left). Differences achieved by different estimator from sine sweep (right).

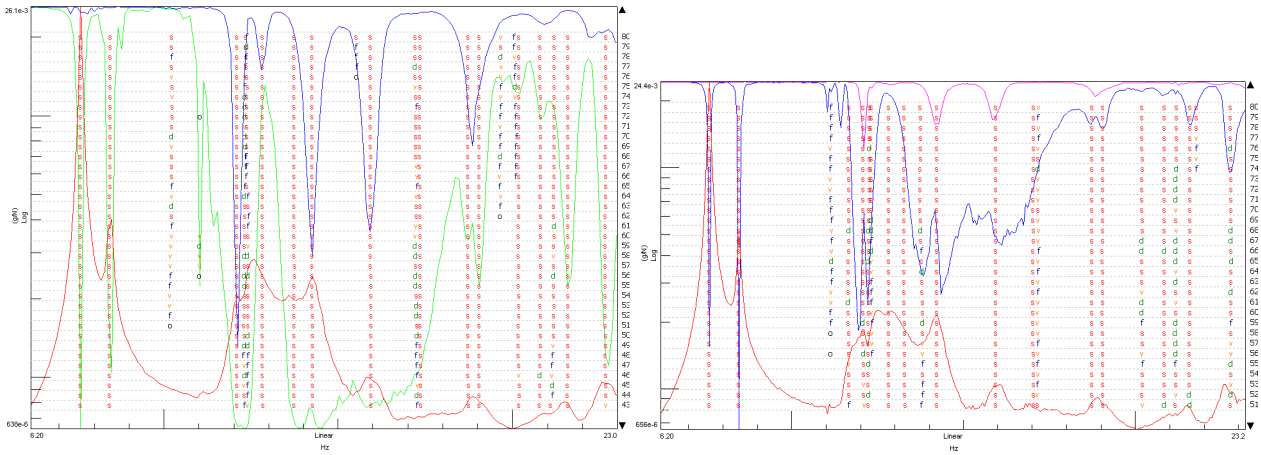

Figure 15: Low frequency stabilization diagram and MvMIF, obtained processing the burst random (left) and sine sweep with DFT (right).

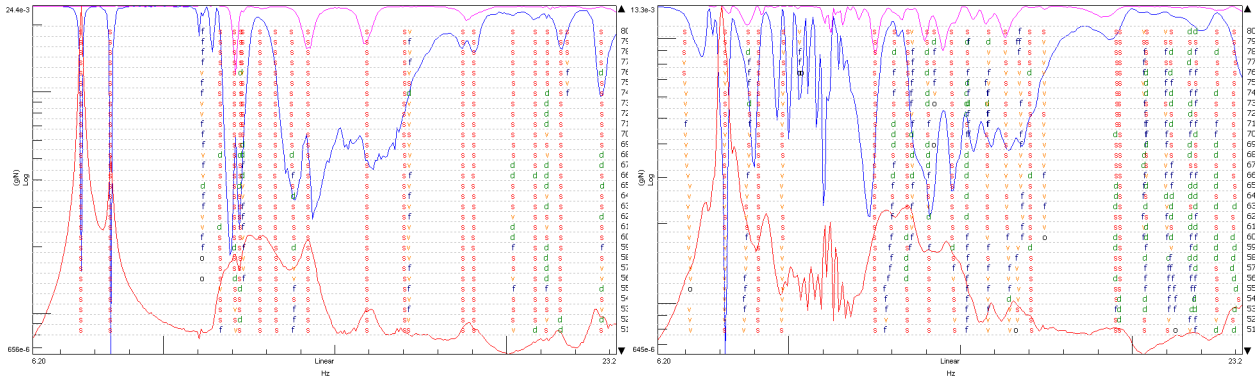

Figure 16: Low frequency stabilization diagram and MvMIF, obtained processing the sine sweep with RDFT (left) and with the harmonic estimator (right).

6 Concluding remarks

In this work different FRF estimators for sine sweep data were compared by analyzing their accuracy in identifying the frequency response functions and the modal parameters. The considered estimation methods are the harmonic estimator, single-block Discrete Fourier Transform (DFT), frequency averaging technique, Welch's method and Reduced Discrete Fourier Transform (RDFT). Two methods emerged on the others: DFT and RDFT. Both estimators are not influenced by the sweep rate. This means that no restrictions for the sweep rate are needed: this can lead to important reduction in time testing. Besides, the direct DFT leads to modal parameters more similar to the theoretical ones with respect to the other methods but the frequency response functions are noisy at high frequency. The RDFT method does not provide any noise averaging, but effectively reduces the very fine resolution from the single-block DFT. Therefore, essentially the same modal parameters are found in both methods. In practice, RDFT yields the frequency response functions and the modal parameters similar to DFT case, but with less computational efforts. In the modal test of large aerospace structures, where typically 100-1000 channels are used [18], the RDFT could be interesting in order to obtain reliable modal data with acceptable computational efforts with respect to the direct DFT method. Although RDFT does not provide an *online* spectrum estimate like the harmonic estimator, the signals can be processed block-by-block during acquisition. From the numerical and experimental investigations it can be concluded that the harmonic estimator yields the worst results in terms of frequency response functions and modal parameters. For this type of estimator, the sweep rate plays an important role because the steady state condition could not be satisfied as the sweep rate increases, specially for low damped structure, leading to distorted FRFs with a consequent wrong identification of the modal parameters.

Acknowledgments

This work was the result of a collaboration between Dipartimento di Ingegneria Aerospaziale e Astronautica of the Università degli Studi "La Sapienza" Roma, and LMS International and was carried out in the frame of the EUREKA project E! 3341 FLITE2. The financial support of the Institute for the Promotion of Innovation by Science and Technology in Flanders (IWT) is gratefully acknowledged.

The authors are also very grateful to Dominique Douessin and Bernard Colomies from SOPEMEA, France, for their hospitality and assistance during the GARTEUR measurements.

References

[1] G. GLOTH, P. LUBRINA. Ground vibration test on the Airbus A380-800, *Proc. IFASD 2005*, Munich, Germany, 2005.

[2] G. GLOTH, M. SINAPIUS. Analysis of swept-sine runs during modal identification, *Mechanical Systems and Signal Processing*, **18**:1421–1441, 2004.

[3] M. BÖSWALD, D. GÖGE, U. FÜLLEKRUG, Y. GOVERS. A review of experimental modal analysis methods with respect to their applicability to test data of large aircraft structures, *Proc. of ISMA 2006*, Leuven, Belgium, 2006.

[4] G. GLOTH, M. DEGENER, U. FÜLLEKRUG, J. GSCHWILM, M. SINAPIUS P. FARGETTE, B.LEVADOUX, AND P. LUBRINA. Experimental investigation of new GVT concepts for large aircraft, *Proc. IMAC 19*, Kissimmee (FL), Feb 2001.

[5] U. FÜLLEKRUG, D. GÖGE. Non-linear analysis of aerospace structure with weak non-linearities and coupled modes, *Proc. IMAC 25*, Orlando (FL), USA, 2006.

[6] W. HEYLEN, S. LAMMENS, P. SAS. *Modal analysis theory and testing*, Department of Mechanical Engineering, K.U.Leuven, 1997.

[7] M. MARCHITTI. Averaging spectral functions from in flight flutter signals, *Mechanical Systems and Signal Processing*, **20**(3):757-761, 2006.

[8] S. PAUWELS, J. MICHEL, M. ROBIJNS, B. PEETERS, J. DEBILLE. A new MIMO sine testing technique for accelerated, high quality FRF measurements, *Proc. IMAC 24*, St. Louis (MO), Jan-Feb 2006.

[9] LMS INSTRUMENTS. *LMS SCADAS III Data Acquisition Front-end*, Breda, The Netherlands, **www.lmsintl.com**, 2008.

[10] LMS INTERNATIONAL. *LMS Test.Lab Structures*, Leuven, Belgium, **www.lmsintl.com**, 2008.

[11] R. PINTELON, J. SCHOUKENS. *System identification: a frequency domain approach*, IEEE Press, 2001.

[12] J. ANTONI, J. SCHOUKENS. A comprehensive study of the bias and variance of frequency-response function measurements: optimal window selection and overlapping strategies. *Automatica*, **43**(10): 1723-1736, 2007.

[13] P. GUILLAUME, P. VERBOVEN, S. VANLANDUIT, H. VAN DER AUWERAER AND B. PEETERS. A poly-reference implementation of the least-squares complex frequency domain estimator, *Proc. IMAC 21*, Kissimmee (FL), USA, February 2003.

[14] B. PEETERS, H. VAN DER AUWERAER, P. GUILLAUME, AND J. LEURIDAN. The PolyMAX frequency-domain method: a new standard for modal parameter estimation? *Shock and Vibration*, **11**, 395–409, 2004.

[15] B. PEETERS. *System identification and damage detection in civil engineering*, PhD thesis, K.U.Leuven, Leuven, Belgium, 2006.

[16] E. BALMÈS, J.R. WRIGHT. Garteur group on GVT – results from the tests of a single structure by 12 laboratories in Europe, *Proc. ASME Design Engineering Technical Conferences*, Sacramento (CA), September 1997.

[17] F. VANHOLLEBEKE, K. VERSTEELE. *Experimental and numerical analysis of the dynamic and Aeroelastic behaviour of a composite aircraft*, MSc Thesis, K.U.Leuven, Leuven, Belgium, 2006.

[18] B. PEETERS, H. CLIMENT, R. DE DIEGO, J. DE ALBA, J. RODRIGUEZ AHLQUIST, J. MARTINEZ CARREÑO, W. HENDRICX, A. REGA, G. GARCÍA, J. DEWEER, J. DEBILLE. Modern solutions for Ground Vibration Testing of large aircraft. *Proc. IMAC 26*, Orlando (FL), USA, 4-7 February 2008.